



Assessing the impact of climate change on high return levels of peak flows in Bavaria applying the CRCM5 Large Ensemble

Florian Willkofer¹, Raul R. Wood^{1,2,3}, Ralf Ludwig¹

¹ Department of Geography, Ludwig-Maximilians-Universität München, Munich, 80333, Germany

5 ² WSL Institute for Snow and Avalanche Research SLF, Davos Dorf, 7260, Switzerland

³ Climate Change, Extremes and Natural Hazards in Alpine Regions Research Center CERC, Davos Dorf, 7260, Switzerland

Correspondence to: Florian Willkofer (florian.willkofer@campus.lmu.de)

Abstract. Severe floods with extreme return periods of 100 years and beyond have been observed in several large
10 rivers in Bavaria in the last three decades. Flood protection structures are typically designed based on a 100-year
event, relying on statistical extrapolations of relatively short observation time series while ignoring potential
temporal non-stationarity. However, future precipitation projections indicate an increase in the frequency and
intensity of extreme rainfall events, as well as a shift in seasonality. This study aims to examine the impact of
climate change on the 100-year flood (HF_{100}) events on 98 hydrometric gauges within the Hydrological Bavaria.
15 A hydrological climate change impact (CCI) modelling chain consisting of a regional single model initial condition
large ensemble (SMILE) and a single hydrological model was created. The 50 equally probable members of the
CRCM5-LE were used to drive the hydrological model WaSiM to create a hydro-SMILE. As a result, a database
of 1,500 model years (50 members x 30 years) per investigated time period was established for extreme value
analysis (EVA) to illustrate the benefit of the hydro-SMILE approach for a robust estimation of the HF_{100} based
20 on annual maxima (AM), and to examine the CCI on the frequency and intensity of HF_{100} in different discharge
regimes under a strong emission scenario (RCP8.5). The results demonstrate that the hydro-SMILE approach
provides a clear advantage for a robust estimation of the HF_{100} using empirical probability on 1,500 AM compared
to its estimation using the generalized extreme value (GEV) distribution on 1,000 samples of typically available
time series size of 30, 100, and 200 years. Thereby, by applying the hydro-SMILE framework the uncertainty from
25 statistical estimation can be reduced. The CCI on the HF_{100} varies for different flow regimes, with snowmelt-driven
catchments experiencing severe increases in frequency and intensity, leading to unseen extremes that impact the
distribution. Pluvial regimes show a lower intensification or even decline. The study highlights the added value of
using hydrological SMILEs to project future flood return levels.



1 Introduction

30 The devastating force of floods poses a significant threat to infrastructure, livestock, and human life. In Germany, two of the most severe floods in the last three decades were the 2002 and 2013 flood events (along with other major events in 1999, 2005, and 2016) (Thieken et al., 2016; Blöschl et al., 2013). The 2002 and 2013 events caused a total of about 17 billion Euros in economic damage due to their large spatial extent and high water levels, with the 2013 flood considered the most extreme event in the last sixty years (Thieken et al., 2016). However, 35 different climatic and catchment conditions caused these events, with the 2002 event resulting from intense rainfall leading to flash floods across multiple small catchments, and the 2013 event due to high antecedent soil moisture from long-lasting precipitation followed by more moderate but spatially widespread rainfall (Thieken et al., 2016). In addition to precipitation intensity, other flood drivers such as antecedent soil moisture conditions, snowmelt, as well as flood driving processes determined by catchment and river characteristics contribute to the non-linearity 40 of the hydrological response to extreme precipitation events (Blöschl et al., 2015). Recent studies analyzing European flood events over the last five decades suggest an increase in the intensity and frequency of high flows and flood events depending on the event type and region (Blöschl et al., 2019; Bertola et al., 2020; Blöschl et al., 2015). However, this trend depends on the time frame considered for the analysis, and the evaluation period remains crucial for either the estimation or the development of high return periods (Blöschl et al., 2015; Schulz 45 and Bernhardt, 2016). Precipitation (heavy precipitation and long-lasting rainfall) and snowmelt (in regions with snowmelt-governed regimes) remain the primary natural causes of flooding, with other influences (e.g., catchment characteristics, antecedent catchment conditions, compound events with snow- or glacier melt) and snowmelt becoming less important once a certain threshold of extreme precipitation is exceeded (Brunner et al., 2021b). According to the sixth Intergovernmental Panel on Climate Change (IPCC) Assessment Report, there is high 50 confidence that a warmer climate will intensify wet weather and climate conditions affecting flooding (IPCC, 2021). Even with a 1.5 °C warming limit under the Paris agreement, heavy precipitation, along with extreme discharge events, is likely to intensify in Europe, with increasing confidence above 2 °C warming (IPCC, 2021). For most discharge gauges, observational records begin in the 19th century or even later (Blöschl et al., 2015). Although most of these observations offer sufficiently long time series of data for estimating peak flows of 55 moderate return periods, they still hinder a robust statistical estimation of extreme return periods, such as the 100-year flood and above. These types of extreme hydrological events are required for structural flood protection and risk management (Wilhelm et al., 2022; Brunner et al., 2021a; Blöschl et al., 2019). Brunner et al. (2021a) illustrate the challenges in modeling and predicting high flows due to data availability, process representation, human influences, and prediction.



60 Recently, single model initial condition large ensembles (SMILE) have emerged as a powerful tool to enhance
statistical analysis of extremes in climatological behavior (von Trentini et al., 2020; Wood and Ludwig, 2020;
Wood et al., 2021; Aalbers et al., 2018; Martel et al., 2020). Unlike other common ensembles of different global
or regional climate model (GCM/RCM) combinations, SMILEs comprise multiple equiprobable realizations
(members) of a single GCM or GCM/RCM combination that differ only in their initial conditions, representing
65 the chaotic nature of the climate system (Arora et al., 2011; Fyfe et al., 2017; Kirchmeier-Young et al., 2017;
Sigmond et al., 2018; Leduc et al., 2019). The actual model structure, physics, parameterization, external forcings
are preserved. Thus, SMILEs offer a profound database for analyzing internal (or natural) climate variability
(Wood and Ludwig, 2020; Martel et al., 2018), separating natural variability from an actual change signal (Aalbers
et al., 2018; Wood and Ludwig, 2020), and extreme events (Wood et al., 2021; Martel et al., 2018). Applying
70 SMILEs for hydrological modelling allows for the creation of a so-called hydro-SMILE, which in turn allows for
the exploitation of vast data for the analysis of the hydrological response of catchments to extraordinary
precipitation events.

This approach of high spatio-temporal resolution for climate and hydrological modelling is computationally
demanding. However, considering spatially refined catchment features (e.g., slopes, soil characteristics, land use),
75 precise values due to higher temporal resolution, and the application of a SMILE for hydrological modelling
supports an enhanced representation of extreme values within models. Thus, this study focuses on the major
Bavarian river basins (upper Danube, Main, Inn) with all their tributaries.

In this study, a climatological SMILE is employed to drive a physically based hydrological model with high spatio-
temporal resolution for the major Bavarian river catchments. The resulting hydro-SMILE is used to answer the
80 following questions:

- a) Is there a benefit applying a SMILE for hydrological impact modelling regarding the estimation of high
flows of large return periods?
- b) How might climate change affect the dynamics in frequency and intensity of extreme discharges?

In this study, we focus on the 100-year flood event to answer both questions. Therefore, the study area is first
85 introduced, followed by an overview of the climatological SMILE post-processing to meet the requirements for
the hydrological modelling. The hydrological model setup used to produce the hydro-SMILE along an evaluation
of its performance are then presented. The subsequent section describes the approaches taken to illustrate the
benefit of a hydro-SMILE for the estimation of peak flow with high return periods and to assess the influence of
climate change on their intensity and frequency. Finally, the results of the analysis are then presented and
90 discussed, followed by concluding remarks.



2 Study Area, Data, and Methods

2.1 Study Area

This study focuses on the major Bavarian rivers, including the upper Danube upstream of Achleiten, Main, Inn, and upstream tributaries of the Elbe, as well as their smaller and larger tributaries originating from adjacent states (Bade-Württemberg, Hessen, Thuringia) and countries (Austria, Switzerland, Italy, Czech Republic). As a result, the catchments of these rivers extend beyond the political borders of Bavaria (Figure 1). The entirety of these catchments is referred to as the Hydrological Bavaria in this study.

The Hydrological Bavaria covers approximately 100,000 km² and features a diverse landscape ranging from the Alps (with the highest point being Piz Bernina at 4049 meters above sea level; m.a.s.l) and the alpine foreland in the south to the southern German escarpment in the north of the study area (with the lowest point being 90 m.a.s.l at Frankfurt-Osthafen) and the eastern mountain ranges to the east (Willkofer et al., 2020; Poschlod et al., 2020). The complexity of these landscapes and different climatological conditions (up to 1100 mm precipitation sums in the north, 2500 mm in the south; an average temperature of 10 °C in the north, down to 5 °C (-8 °C on alpine summits) in the south results in a variety of runoff regimes (Poschlod et al., 2020).

The discharge of many rivers within the Hydrological Bavaria is influenced by artificial retention structures (i.e., dams, retention basins), naturally formed lakes, or transfer systems (drinking water supply, low flow elevation) (Willkofer et al., 2020). The major river catchments were divided into a total of 98 smaller sub-catchments based on a common interest in flood protection and a more detailed variation in catchment characteristics, using a selection of gauges (Willkofer et al., 2020).

110

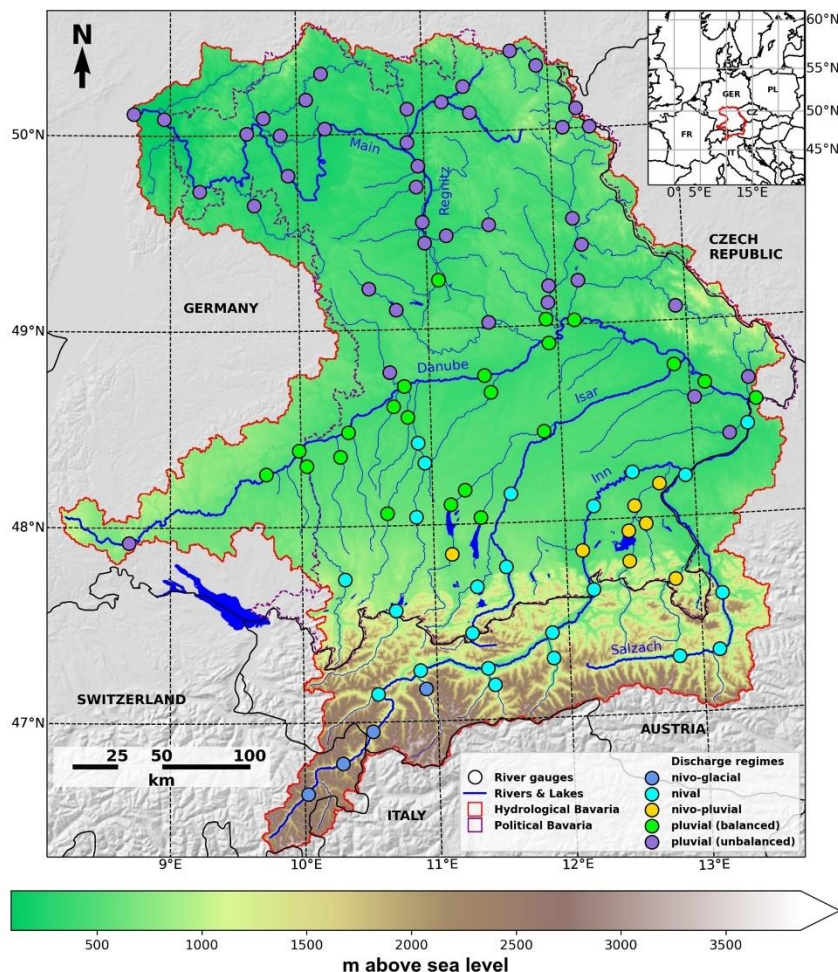


Figure 1: Map showing the elevation of the Hydrological Bavaria (red line) which comprises the political Bavaria (dashed purple line) and the 98 hydrometric gauges used in this study as well as their respective discharge regime type (colored dots) at their respective rivers (blue lines).

115 2.2 Data and Methods

To assess the impact of climate change on extreme return periods of peak flows, the hydroclimatic modeling chain illustrated in Figure 2 was introduced within the scope of the ClimEx project (Climate Change and Hydrological Extreme Events, www.climex-project.org). This common chain is divided into a climate and a hydrological impact section and covers three spatial scales (GCM scale, RCM scale, hydrological model scale) with increasing resolution along the chain.

120

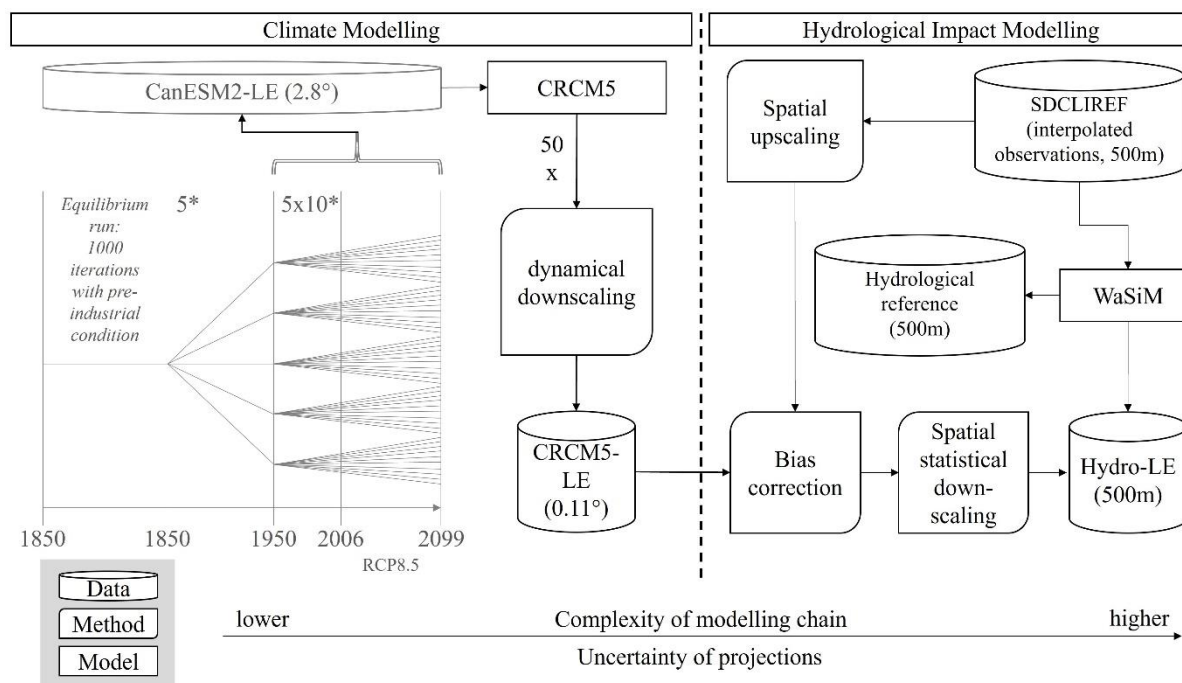


Figure 2: The ClimEx modelling chain uses the CanESM2 large ensemble (LE, gray, not created within the ClimEx project) to generate the CRCM5-LE. The CRCM5-LE is then used to explore the impacts of climate change on the hydrology of the Hydrological Bavaria through a hydrological large ensemble (Hydro-LE). The CRCM5-LE represents a SMILE, consisting of a single model that downscales output from the employed ESM using slight differences in the initialization.

125

Since the introduced model chain requires a vast number of computational resources, the ClimEx project employed the high-performance computing systems of the Leibniz Supercomputing Centre (LRZ) as well as its technical and consultative support to migrate and adapt software and data to its systems, facilitate calculations, and provide an extensive amount of storage to archive the data and make them available to the scientific community (data available at <https://www.climex-project.org>).

130

2.2.1 Climate data

A SMILE composed of 50 independent members of the Canadian Earth System Model, version 2 (CanESM2) large ensemble (LE) was used as a base for all further analysis. The CanESM2-LE was produced by the Canadian Centre for Climate Modelling and Analysis (CCCma) and described in previous publications (Fyfe et al., 2017; Kirchmeier-Young et al., 2017; Arora et al., 2011; Leduc et al., 2019). All members of the CanESM2-LE used natural and anthropogenic forcings for the historical period from 1950 to 2005 and the representative concentration pathway 8.5 (RCP8.5; van Vuuren et al., 2011) emission scenario from 2006 to 2099 (Kirchmeier-Young et al.,

135



140 2017; Leduc et al., 2019; Fyfe et al., 2017; Sigmund et al., 2018). The individual members differ only in their initial conditions rather than changes in model structure, physics, or parameters, and therefore offer a range of internal or natural variability of the climate system at a global scale.

145 These 50 members were dynamically downscaled from $\sim 2.85^\circ$ (T63; ≈ 310 km) to 0.11° (≈ 12 km) using the Canadian Regional Climate Model, version 5 (CRCM5; Martynov et al., 2013; Šeparović et al., 2013) over two spatial domains, the European and the northeastern North American domains (Leduc et al., 2019). As with the CanESM2-LE, variations between the individual members were obtained by unique initial conditions for each member, thus providing a range of internal or natural variability on a regional scale. The resulting CRCM5 large ensemble (CRCM5-LE; Leduc et al., 2019) of 50 transient members provides the basis for assessing the impact of climate change on hydro-meteorological extreme events for the Hydrological Bavaria. Furthermore, the individual members of the CRCM5-LE are considered independent for the hydrological evaluation period from 1981 to 2099, as the analysis of variations in temperature and precipitation over land and ocean shows (Leduc et al., 2019). A comparison between the CRCM5-LE and the E-OBS observational gridded dataset (Haylock et al., 2008) at the CRCM5 grid revealed biases for a historical period between 1980 and 2012, showing regional and seasonal variations in magnitude over Europe (Leduc et al., 2019).

155 Since this bias was considered to affect the behavior of the outputs of the hydrological model due to shifts in seasonality and intensity, a bias correction was applied. The required meteorological data of precipitation, air temperature, relative air humidity, incoming shortwave radiation, and wind speed were adjusted to a meteorological reference of interpolated 3-hourly station data (Sub-Daily Climate Reference, SDCLIREF; Ludwig et al., 2019) on the RCM scale using an adaptation of the quantile-mapping approach after Mpelasoka and Chiew (2009). This approach as described in Willkofer et al. (2018) involved using multiplicative or additive correction factors, and was further adapted for using 3-hourly correction factors for every quantile and month. To preserve an internal spread between the members, a single set of factors was deduced from a combination of all 50 members. Despite bias correction being often considered inevitable for climate change impact studies (Gampe et al., 2019), numerous studies argue about the benefits (increasing reliability of climate change projections of the hydrological impact model, reducing bias in mean annual discharge) and shortcomings (disrupting feedbacks between fluxes, modification of change signals, assumption of a stationary bias) of its application for hydrological climate change impact studies (e.g., Teutschbein and Seibert, 2012; Maraun, 2016; Ehret et al., 2012; Dettinger et al., 2004; Chen et al., 2021; Huang et al., 2014).

170 Subsequently, the bias corrected data were statistically downscaled to the hydrological model scale (500×500 m²) using a mass preserving approach. This approach involved the spatial interpolation (inverse distance weighting) of anomalies for each time step from the monthly mean state (1981-2010) for each of the CRCM5-LE cell center



points to the hydrological model scale (Brunner et al., 2021b). The interpolation result was then applied to the SDCLIREF reference fields (Brunner et al., 2021b).

For further details, readers are referred to a comprehensive summary in the Supplementary Materials for the CanESM2-LE (S1), the CRCM5-LE (S2), the bias correction (S3), and spatial downscaling method (S4).

175 **2.2.2 Hydrological Model WaSiM**

The Water balance simulation Model (WaSiM; Schulla, 2021) was employed to perform the hydrological simulations driven by the CRCM5-LE resulting in a hydro-SMILE (the WaSiM-LE). WaSiM is a distributed, mostly physically-based, and deterministic model for simulations on various spatial (1 m to 10 km) and temporal (minute to daily) scales with a constant time step. It includes routines for evapotranspiration, snow accumulation and melt, glaciers, soil water transfer, groundwater, discharge generation and routing (Schulla, 2021). The model is frequently used for hydrological climate change impact studies for small-scale to mesoscale catchments on various topics, such as glaciers, groundwater, and discharge (Iacob et al., 2017; Neukum and Azzam, 2012; JÓNSDÓTTIR, 2008).

The model was set up in high spatio-temporal resolution (500 m and 3 h) for 98 catchments of the Hydrological Bavaria with a focus on high flow representation using distributed data derived from the European DEM (EU-DEM; European Environment Agency, 2013b), land use data provided by the CORINE land cover dataset (European Environment Agency, 2013a), distributed soil information from the European Soil Database (ESDBv2.0; European Environment Agency, 2013a), as well as groundwater information provided by the Hydrogeologische Übersichtskarte (HÜK; Dörhöfer et al., 2001) and IMHE (IHME; BGR, 2014). A single set of parameters for distributed parameters (i.e., evapotranspiration, soil properties) was defined globally for the entire modeling domain (Willkofer et al., 2020). Local parameters for discharge storage components (i.e., interflow, direct flow) were calibrated using an automated algorithm (dynamically dimensioned search (Tolson and Shoemaker, 2007) and simulated annealing with progressing iterations (Černý, 1985; Kirkpatrick et al., 1983)) minimizing a weighted combination of performance metrics, including Nash and Sutcliffe efficiency (NSE; Nash and Sutcliffe, 1970), Kling-Gupta efficiency (KGE; Gupta et al., 2009), the logarithmic NSE and the ratio of root mean squared error to standard deviation (RSR; Moriasi et al. (2007)) (Eq. (1)) (Willkofer et al., 2020). Due to the focus on high flow representation more emphasis was placed on the respective measures (i.e., NSE and KGE). For further details about the model setup the reader is referred to Willkofer et al. (2020). The overall metric (OM) is defined as follows:

$$200 \quad OM = 0.5 \times (1 - NSE) + 0.25 \times (1 - KGE) + 0.15 \times (1 - \log NSE) + 0.1 \times RSR \quad (1)$$



The simulations of a single parameter set for various catchments within a heterogeneous landscape revealed satisfactory to very good results for most of the 98 gauges during the 30-year reference period of 1981 to 2010. However, for a few gauges (NSE: 16; KGE: 5), the model was not able to reproduce the observed discharge satisfactorily (values below 0.5) (Willkofer et al., 2020; Poschlod et al., 2020). Furthermore, the simulations reproduced the mean high flow sufficiently well, with over 60% of the gauges showing absolute deviations from observed values below 20%. Nonetheless, gauges in alpine or pre-alpine catchments exhibited a deficit in mean high flow values due to the lack of observed precipitation resulting from an undercatch of precipitation for that region (Poschlod et al., 2020). Consequently, the level of trust (LOT) for peak flows of return periods of 5, 10, and 20 years flood events, introduced in Willkofer et al. (2020) showed a moderate to high confidence for most catchments, with gauges of poor simulated performance yielding a lower LOT with increasing return levels. LOT were not provided for extreme flood events (i.e., 100-year flood events) since they are subject to significant epistemic uncertainty due to the restricted availability of simulated data (30 years).

The resulting hydro-SMILE comprises 50 members of transient simulated data from 1961 to 2099, providing a total of 6,950 model years to be exploited to analyze extreme values. The entire modelling period is shortened by ten years to account for the time span it takes the RCM to produce fully independent realizations due to the inertia of the ocean model (Leduc et al., 2019).

2.2.3 Benefit of a hydro-SMILE for the estimation of extreme peak flows

This study used the simulated discharge for the reference period of 1981 to 2010 out of the entire dataset to assess the benefits of the hydro-SMILE in estimating return levels. Similar to the individual members of the CRCM5-LE, the members of the WaSiM-LE are equally probable and, therefore, provide a comprehensive database to facilitate the analysis of extreme values.

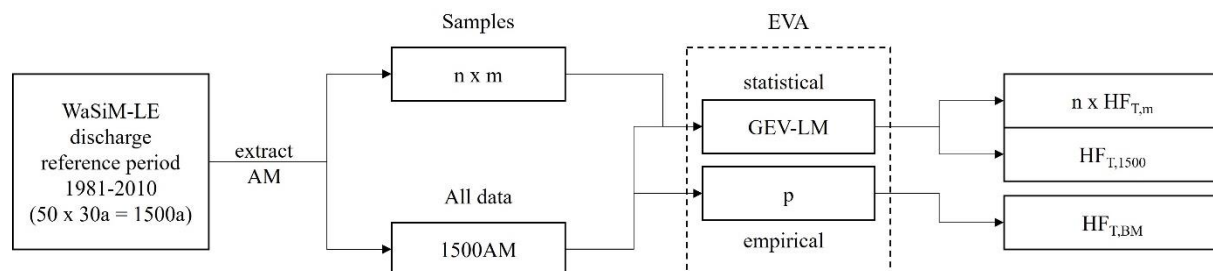


Figure 3: Process chain illustrating the benefit of a hydro-SMILE for climate change impact studies on peak flows of extreme return periods. The process includes extreme value analysis (EVA) based on annual maximum (AM), with bootstrapping resampling to create n different samples of sample size (m). The probability of non-exceedance (p) and the Generalized Extreme Value (GEV) distribution with the L-Moments (LM) estimators are used to derive estimates for high flow values of the return period T (HF_T). The statistical analysis was performed using the extRemes package (v2.0) for R (Gilleland and Katz, 2016).

225

230

235

240

245

250

Figure 3 illustrates the approach taken to emphasize the benefits of the hydro-SMILE in analyzing peak flows of high return periods for the reference period. The 30-year reference period (ref) was selected for all 50 members, resulting in 1,500 model years (50 members \times 30 years) of discharge data for each of the 98 gauges. First, the annual maximum of each model year (hydrological year) was extracted for the analysis. Since the database consists of 1,500 model years, this number is considered sufficient to employ empirical non-exceedance probabilities (Martel et al., 2020). However, to demonstrate the benefit of the hydro-SMILE database a statistical analysis using the stationary Generalize Extreme Value (GEV) distribution was also conducted for comparison purposes. A bootstrapping approach with resampling was used to create 1,000 samples (n) of different sizes m (30, 100, 200) years (each sample without replacement). Using 1,000 samples ensures that one value of the 1,500 AM has a chance of $>99\%$ of being selected by chance for $m = 30$. The GEV was employed to estimate the return periods and corresponding confidence intervals. The parameters of the GEV distribution were estimated using L-Moments. The GEV distribution was selected as it is among the better performing methods relying on AM (Bezak et al., 2014) and is the recommended choice for German gauges (Salinas et al., 2014; Fischer and Schumann, 2016). Although the sample size of 30 and 100 AM may be small for estimating peak flows of high return periods, they were selected along with a size of 200 AM as they represent an average (30 years) to rare (100 & 200 years) data availability of observed discharge values at different gauges (GRDC, 2021). The resulting 1,000 estimates for return levels of peak flows offer a comprehensive database to demonstrate the benefit of the hydro-SMILE. Additionally, the GEV was calculated using the entire 1,500 AM database for each gauge to allow for a comparison with a benchmark value. This benchmark for the return levels of peak discharge was deduced by applying the quantile based on the empirical probability of non-exceedance p (Eq. (2)) to all 1,500 AM values for each gauge, and it is considered to represent a robust estimate. This analysis focused on the 100-year flood, which is an event



of a 100-year return period T (HF_{100} ; $T = 100$) and the corresponding 99th percentile p of the distribution of the 1,500 AM values as a benchmark.

$$p = 1 - \frac{1}{T} \quad (2)$$

255 Values for the benchmark derived by the empirical probability as well as the HF_{100} values estimated using the GEV are further normalized to the benchmark to allow for a better comparison.

2.2.4 Projection of changes in frequency and intensity

This study further investigates the dynamics of intensity and frequency of the HF_{100} for three future periods (near future: 2020-2049; mid future: 2040-2069; far future: 2070-2099). Therefore, the robust estimates of extreme return levels of peak flows derived by the empirical probabilities are used for the assessment of climate change
260 impacts on their intensity (C_I , Eq. (3)) and frequency (C_F , Eq. (4a to c)) in the three future periods.

$$C_I = \left(\frac{HF_{T_{fut}} - HF_{T_{ref}}}{HF_{T_{ref}}} \right) \cdot 100 \% \quad (3)$$

$$C_F = \frac{1}{1 - f(HF_{T_{ref}})} \quad (4a)$$

$$f = F(HF_{T_{fut}}) \quad (4b)$$

$$F(x) = \sum_{i=1}^j h_i = \sum_{i=1}^j \frac{h(x_i)}{n} \quad (4c)$$

265 The change in intensity is given as the difference between the future ($HF_{T_{fut}}$) and reference value ($HF_{T_{ref}}$) relative to the reference value in percent. The change in frequency is expressed as the return period value T and is calculated by applying the empirical cumulative distribution function F (ECDF with frequency for an event h_i described as the ratio between the frequency for the specific event $h_{(x_i)}$ and the number of all values n , Eq. (4c)) for the respective future period (f , Eq. (4b)) to the value of the 100-year flood of the reference period (Eq. (4a)). The percentile value
270 of f for the reference 100-year flood value is then used to deduce the future return period by solving the empirical probability of non-exceedance for the return period T (Eq. (4a)). The change signals are calculated for each of the above mentioned 30-year future periods. However, this analysis requires stationarity for the underlying data. Since we use the entire 1,500 model years provided by the 50 members, we determine stationarity if less than 5 % of the members exhibit a significant trend for each individual gauge. A Mann-Kendall (MK) test for stationarity
275 conducted on each individual member and gauge revealed no significant trend for the reference period (with significance level $\alpha = 0.01$) for more than 95 % of the members along all gauges. However, for the future periods the MK test exhibits significant trends for more than 5 % of the members in 6 of the 98 gauges. Limiting the



280 evaluation periods to 20 years instead of 30 years lead to similar results for the MK test showing no apparent trend for all gauges in the reference period, but showing for at least one gauge a significant trend (more than 5 % of members with a trend) in the future periods. Studies by Poschlod et al. (2020) and Brunner et al. (2021b) conducted their analysis on the same database using time slices of at least 30 years as well. Thus, we choose to use 30-year periods since stationarity criteria are met in most catchments and opt for the larger database, as well as maintaining consistency with these studies.

3 Results

285 3.1 Benefits of hydro-SMILEs for the estimation of extreme return periods of peak flows

Large ensembles provide a vast amount of data, therefore they are considered to be beneficial for extreme value analysis (Kendon et al., 2008; Kjellström et al., 2013; Wood and Ludwig, 2020). The benefit of a hydro-SMILE to determine robust extreme hydrological discharge values for Hydrological Bavaria are analyzed, specifically for the 100-year flood. The robust values for the discharge gauges, derived using the empirical probability of non-exceedance for a 100-year event, serve as a benchmark for comparison with values derived by the GEV distribution using three different sample sizes (30, 100, 200) of AM values (Figure 4).

The results shown in Figure 4 (a, b, and c) illustrate that the estimates of HF_{100} are more robust with an increasing number of AM values used for the GEV, as indicated by the spread of the blue markers around the black benchmark line. Table 1 summarizes the statistical characteristics of the deviation of the estimates from the benchmark across all 98 gauges. While the range of the relative deviation of the 1,000 samples of HF_{100} estimates from the benchmark is between 0.33 and 2.71 when calculated with a sample size of 30 AM values (panel a), this range diminishes to 0.49 and 1.91 for 100 AM values (panel c) and 0.56 and 1.60 for 200 AM values (panel e). Therefore, the range of the 1,000 estimates diminishes with an increase in sample size and the values cluster more densely around the benchmark. However, despite the remaining non-negligible range of deviations from the benchmark, the mean (1.01) as well as the median (0.98 to 1.0) across all values for all gauges are close to the benchmark value for different sample sizes. The inner 50 % of the 1000 samples across all 98 gauges exhibit the largest deviation with a sample size of 30 AM (between 0.84 and 1.15) and the lowest for 200 AM (0.94 to 1.07). Therefore, only 25 percent of the samples show underestimations below 0.84 (0.92, 0.94) and only 75 percent exhibit larger overestimations than 1.15 (1.08, 1.07) with a sample size of 30 AM (100 AM, 200 AM). Thus, with deviations larger than 15 % for 50 percent of the estimates calculated using a sample size of 30 AM, only half of the estimated HF_{100} values are within an acceptable range ($\pm 15\%$, considering model parameter uncertainty and errors in

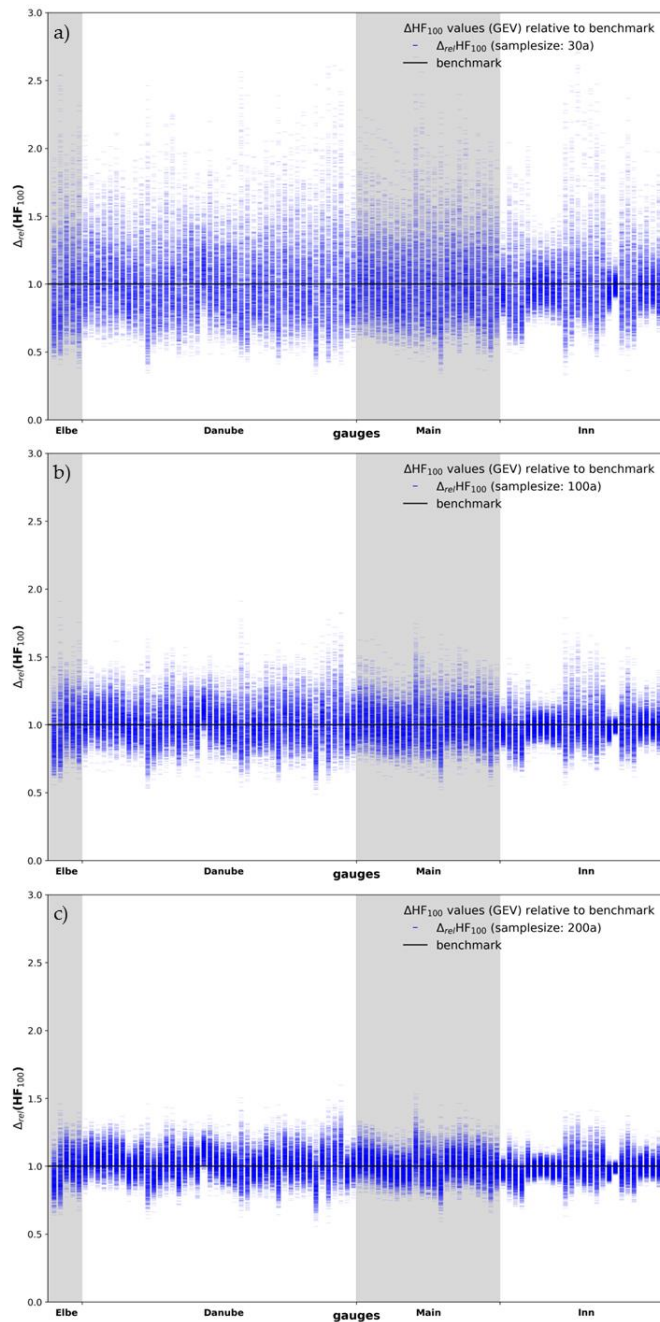


observations affecting the model quality regarding high flows) compared to the benchmark. This number increases with a larger sample size.

310 **Table 1: Summary of overall statistics of the relative deviation of the HF₁₀₀ estimates from the benchmark value across all gauges. The table includes the number of sample (n), sample size (m) given in annual maximum (AM) values and the 0.25/0.75 quantile (Q25, Q75) values.**

n	m	minimum	Q25	mean	median	Q75	maximum
1000	30	0.33	0.84	1.01	0.98	1.15	2.71
1000	100	0.49	0.92	1.01	1.00	1.08	1.91
1000	200	0.56	0.94	1.01	1.00	1.07	1.60
1	1500	0.98	1.00	1.02	1.01	1.03	1.09

315 While the majority of gauges show estimates that are evenly distributed around the benchmark, some gauges exhibit a tendency towards over- or underestimation of the HF₁₀₀ estimates with more values falling above or below the benchmark line. This behavior may be different when using more than 1000 samples to conduct the analysis. The difference between the benchmark value obtained from empirical probability and the estimates obtained from the GEV distribution can vary greatly depending on the samples selected from 1,500 AM values.

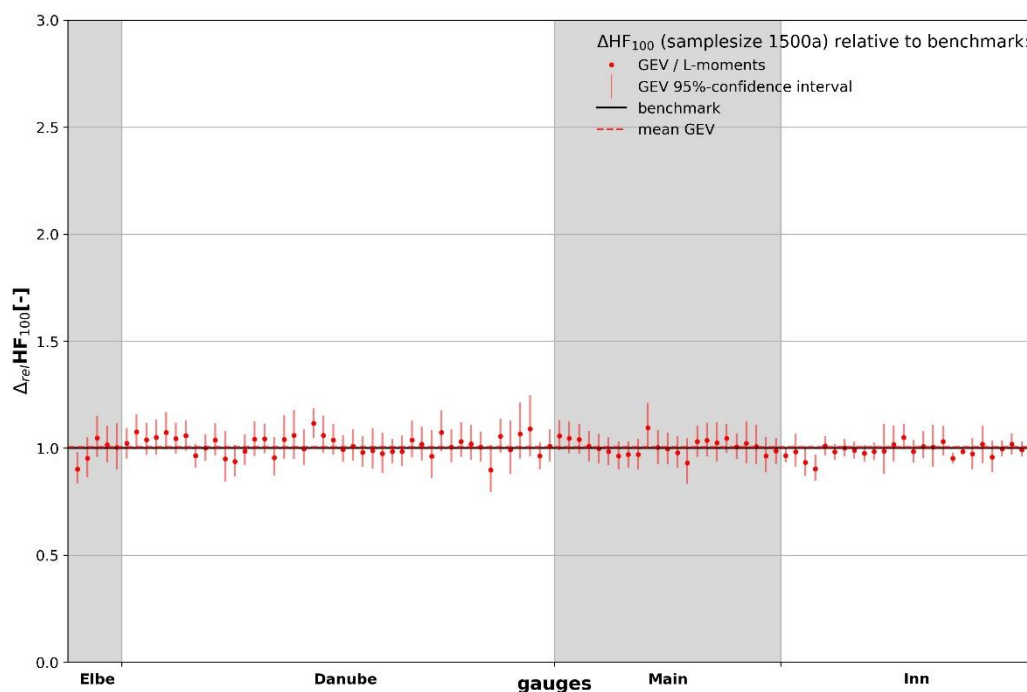


320 **Figure 4: Comparison of HF₁₀₀ estimates calculated using the GEV distribution with 1000 AM samples of a) 30, b) 100, and c) 200 years per gauge (blue markers) with the respective benchmark value (solid black line) for 98 gauges.**



325

In Figure 5, a comparison is made between the HF_{100} estimates derived using the empirical probability of non-exceedance and those obtained using the GEV distribution (and associated 95 % confidence intervals) for the entire ensemble of 1,500 AM values. The robust values obtained from the empirical probability are used as the benchmark for this comparison.



330

Figure 5: Relative difference of the HF_{100} values (red dots) and respective 95th confidence intervals (vertical red lines) calculated with the GEV distribution from the benchmark HF_{100} value (black solid line) derived from the probability of non-exceedance $p = 0.01$. The results are based on the entire reference database of 1500 AM values for each of the 98 gauges. The horizontal red dashed line illustrates the mean of relative difference the HF_{100} calculated with the GEV distribution for the 98 gauges.

335

The estimates obtained using the GEV show differences from the benchmark, with varying magnitudes across the gauges. However, the mean difference across all HF_{100} estimates is small and marginally different from the benchmark. For most gauges, the individual differences from the benchmark are also small, with only two gauges showing values exceeding $\pm 10\%$. However, for 7 of 98 gauges the 95 % confidence interval does not overlap with the benchmark, indicating that in this case the empirical approach yields a more robust value compared to the GEV estimates even with the enhanced robustness gained by employing 1,500 AM values as a sample. However, if the unknown population could be represented by the GEV, the distribution would yield a better fit. Therefore, the determination of peak flows with extreme return periods employing the empirical probability on the vast data base of a hydro-SMILE allows for a more precise estimation. Hence, also the estimation of future return periods is more

340



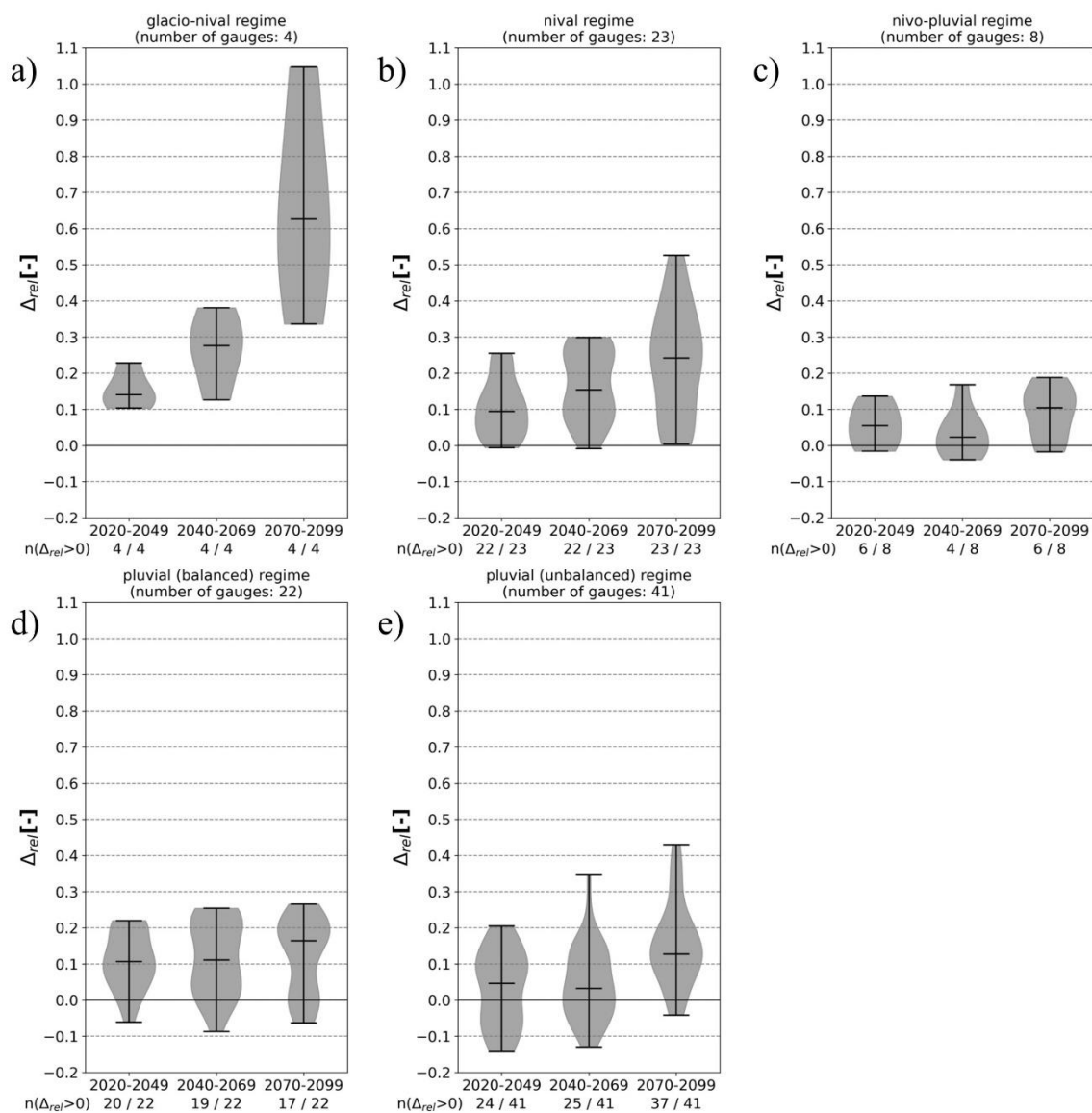
robust allowing for a better quantification of the changing dynamics in the frequency and intensity of high return periods in future projections due to changes in the climate.

3.2 Changing dynamics of the 100-year peak flows in future projections

345 The changes in 100-year peak flows (HF_{100}) for the investigated gauges in Hydrological Bavaria in the 21st century are summarized for five distinct discharge regimes (defined by the Pardé coefficient) which were adapted from Poschlod et al. (2020) (Figure 1). One gauge that was originally assigned to its own regime has been re-allocated to the pluvial (unbalanced) regime, as it exhibits a similar mean discharge behavior. The regimes comprise the glacio-nival regime of four high Alpine catchments, a nival regime of mostly Alpine to pre-Alpine catchments, a nivo-pluvial regime of pre-Alpine catchments, a balanced pluvial regime along the Danube and its tributaries in
350 the Alpine foreland, and the unbalanced pluvial regime.

Within the study area, the flood protection structures are typically designed based on a stipulated estimation of HF_{100} from observations, which represent a stationary condition in the past. Any future increase in the intensity and frequency of these extreme values poses a threat to these structures. Therefore, the following graphs highlight the changes of the HF_{100} events for the three future periods.

355 Figure 6 displays violin plots that illustrate the range of changes in the intensity of HF_{100} events for the different discharge regimes as well as the distribution of changes across the respective clusters of gauges for the near (horizon 2035), mid (horizon 2055), and far future (horizon 2085) periods. Overall, 78 % of all gauges (76/98) show an increase in intensity for the 2035 horizon, 76 % (74/98) for the 2055 horizon, and 89 % (87/98) for the 2085 horizon.



360

Figure 6: Violin-plots indicating the changes of the intensity of the HF₁₀₀ for the three future periods (near, mid, far) compared to the reference period, with changes presented as relative difference (Δ_{rel}) between the reference and the future HF₁₀₀ value for each gauge. Results of the 98 gauges are aggregated for the five discharge regimes (a = glacio-nival, b = nival, c = nivo-pluvial, d = pluvial (balanced), e = pluvial (unbalanced)). The figures display the total number of gauges per regime as well as the number of gauges depicting an increase in intensity.

365

The CCI are most severe for the glacio-nival regime (Figure 6a), as all three future periods exhibit an increase in intensity of the HF₁₀₀ events of at least 10% compared to the reference period. The nivo-pluvial regime (Figure 6c) shows the smallest spread and the lowest increase in HF₁₀₀ intensity across all future periods compared to the



reference period. As the distance from the Alps increases and the discharge regimes shift from snowmelt influenced
370 to more precipitation driven, the number of gauges projecting a decrease in HF_{100} intensities increases. However,
the majority of gauges still exhibit an increase in intensities, with up to 18.8% for the nivo-pluvial (Figure 6c),
26.6% for the balanced pluvial (Figure 6d), and 43 % for the unbalanced pluvial regime (Figure 6e) in the far
future. The gradient of an increase in intensity over all three projection periods is small for the nivo-pluvial and
balanced pluvial regimes, which show the least intensification of HF_{100} values for the respective periods. However,
375 the gradient of increase is more distinct for the remaining regimes, with the largest increase in the glacio-nival
regime (Figure 6a). The gauges in this regime depict the strongest increase in HF_{100} intensities for the 2085 horizon,
with an increase of 36.6 % to 104.7 %.

Based on the future projections of the hydro-SMILE, the discharge values of the HF_{100} are likely to increase for
most of the gauges of Hydrological Bavaria. Consequently, the frequency of the HF_{100} discharge for the reference
380 period also increases. Figure 7 shows the change in frequency between the future and the reference period for the
different regimes.

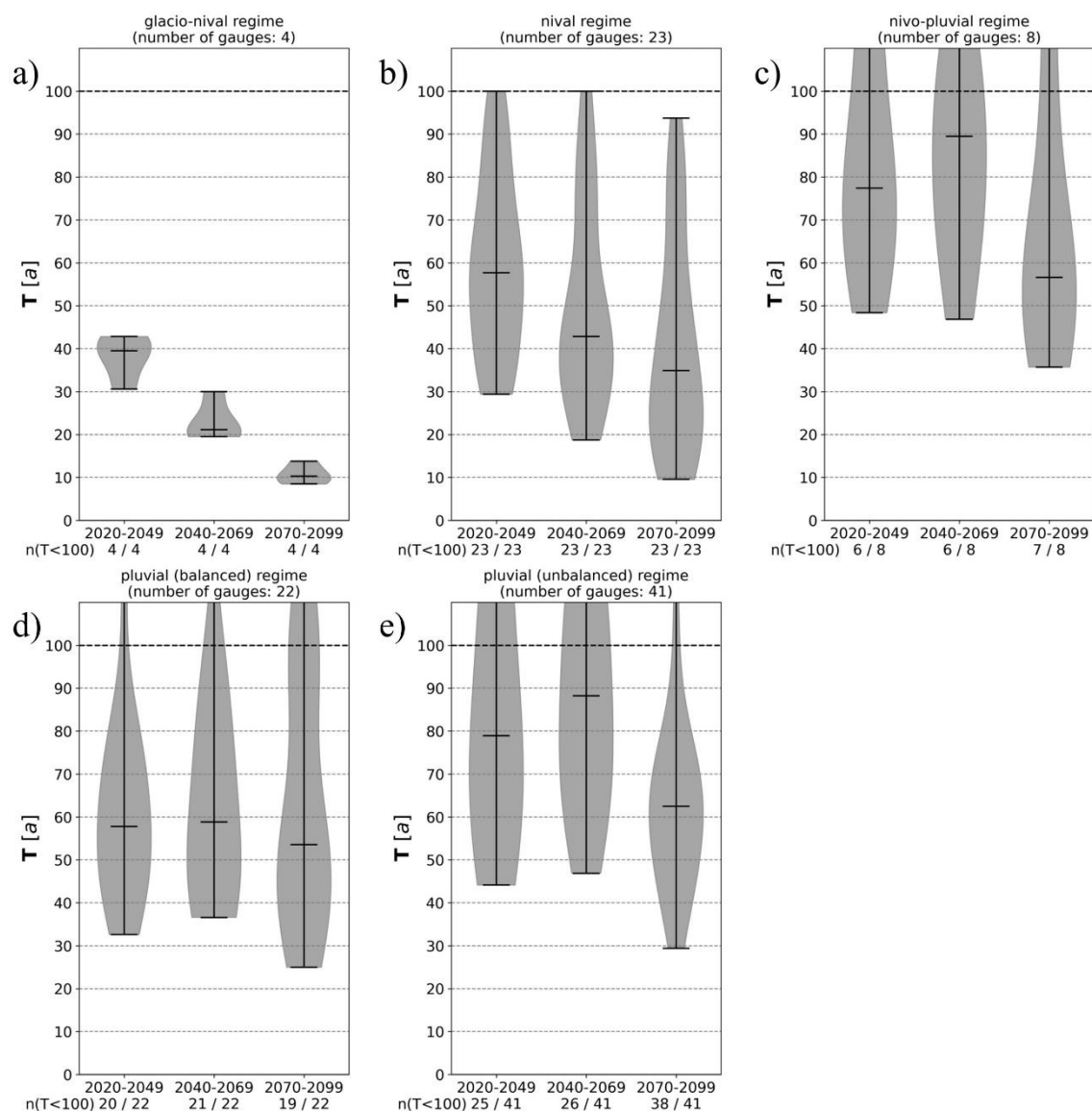


Figure 7: Violin-plots indicating the changes of the frequency of the HF_{100} for the three future periods (near, mid, far) compared to the reference period, with changes presented as absolute values of return periods (T [a]) of the respective future period compared to the 100-year return period for each gauge. Results of the 98 gauges are aggregated for the five discharge regime (a = nivo-glacial, b = nival, c = nivo-pluvial, d = pluvial (balanced), e = pluvial (unbalanced)). The figures display the total number of gauges per regime as well as the number of gauges depicting an increased frequency.

385

Values indicate the new return period associated with the HF_{100} discharge from the reference period. This means values below 100 indicate an increase in frequency. The glacio-nival regime (Figure 7a) also exhibits the strongest increase in frequency among all regimes with the HF_{100} of the past becoming equivalent to a 31- to 43-year event

390



in the near future, thus becoming roughly two to three times more frequent. For the 2085 horizon the same HF₁₀₀ event becomes an 8- to 14-year event showing a seven to twelve-fold increase in frequency. A similar development is visible for some gauges in the nival regime (Figure 7b). While the violin plot for this regime indicates that the reference 100-year event will become a 70-year event for more than 50% of gauges, some gauges show no or only
395 a minor increase in frequency as well. The changes for the remaining regimes are less severe, but still indicate an increase in frequency for up to 50 % of the respective gauges until the middle of the century and more than 50 % in the far future. The changes for the nivo-pluvial regime (Figure 7c) and the unbalanced pluvial (Figure 7d) regime show that the frequency declines for less than 50 % of the gauges in the near and mid future period. Therefore, the 100-year event becomes more frequent for more than 50 % of the gauges with varying extent. While the magnitude
400 of changes is similarly moderate (except for the far future) for Figure 7c and Figure 7e, projected future return periods for the HF₁₀₀ event for Figure 7d depict stronger change signals towards higher frequencies with more than 50 % of gauges showing values smaller than 60 years. Furthermore, the nivo-pluvial as well as the balanced and unbalanced pluvial regimes exhibit a slight decrease in frequency in the mid future compared to the remaining projection periods while the intensity does not show this behavior. However, this circumstance may be explained
405 by the change in driving agent from snowmelt driven events in the near future to rainfall induced events at the end of the century. Thus, at the 2055 horizon the shift of the ratio of both event types contributes to this slight decline in frequency.

Some gauges within the nivo-pluvial and both pluvial regimes depict a decrease in frequency and/or intensity. These gauges usually exhibit natural or artificial influences, such as the retention effect of natural lakes, reservoirs,
410 or diversions or gauges of small catchments which might experience less dynamics in changes of flood drivers or even a reduction.

Overall, the changes in frequency and intensity due to the projected changes in climate according to the CRCM5-LE become less severe with increasing distance from the Alps. Furthermore, the increase in frequency and intensity for alpine catchments is seemingly high, but in line with the results of Hattermann et al. (2018), which showed
415 comparable results for the near future period (100-year event frequency between 20 and 40 years). The influencing factors for these in parts severe changes are manifold. However, Brunner et al. (2021b) analyzed the relation between the extremeness of precipitation and discharge for 78 out of the 98 gauges within Hydrological Bavaria and concluded that an increase in extreme precipitation intensity is of higher importance for extreme return levels of discharge than land surface processes, such as antecedent soil moisture or changes in snowpack due to warmer
420 temperatures. If precipitation volumes are sufficiently large, they quickly saturate the soil or yield an excessive amount of direct runoff due to infiltration excess (Brunner et al., 2021b).



The mean magnitude of the annual maximum precipitation is projected to change for different temporal aggregation levels (3-hourly to 5-daily) in the CRCM5-LE (Wood and Ludwig, 2020), as well as the magnitude of 100-year return period rainfall increases by 10-20% and the frequency increases by 2 to 4 times (Martel et al., 2020) for Hydrological Bavaria. The changes are associated with seasonal shifts from summer to winter events and are particularly pronounced in the Alpine region (Martel et al., 2020; Wood and Ludwig, 2020). Severe floods that occur simultaneously in different catchments of the study area are usually associated with a cutoff low Vb cyclone that results in prolonged precipitation events lasting up to 15 days over the same region (Stahl and Hofstätter, 2018; Mittermeier et al., 2019). Under changing climate conditions projected by the CRCM5-LE by the end of the 21st century employing the RCP8.5 scenario, these events are likely to intensify in volume and frequency during winter and spring and occur less frequently during the summer months but with an increased precipitation volume (Mittermeier et al., 2019).

4 Discussion

The variability of statistical characteristics within a time series can affect the estimation of extreme values due to extraordinary events (Fischer and Schumann, 2016). The results of this study emphasize the benefit of using data provided by a climatological SMILE for hydrological impact studies as it provides a profound basis for extreme value statistics and allows for more accurate estimation of extreme values, as also shown by other studies (Champagne et al., 2020; Ehmele et al., 2020; Maher et al., 2021). However, the in parts large deviations between the benchmark (robust estimate derived from the empirical probability for a 100-year flood event using 1,500 AM values) and the estimates derived using a GEV based on different sample sizes (30, 100, 200) might be reduced when using an EVD which is better suited for the respective sample when enough data is available (as is the case with hydro-SMILE used here). In some cases the GEV might not be the best distribution for the samples of the respective gauge which might affect the differences from the benchmark since higher quantiles heavily depend on the distribution (Schulz and Bernhardt, 2016). However, the approach presented in this study illustrates the benefit of a hydro-SMILE as it provides a more robust estimate by employing empirical probabilities for the deduction of extreme values. Therefore, these robust estimates allow for a more robust assessment of future dynamics of extreme high flows.

The results of this study are subject to uncertainties (parameter, process description) as they are produced by data created at the end of a cascade of modeling steps usually applied for climate change impact studies as displayed in Figure 2. Different components (e.g., climate model, hydrological model, bias correction) affect different discharge characteristics or indicators (e.g., extreme indicators, mean discharge) (Gampe et al., 2019; Muerth et



al., 2012; Muerth et al., 2013; Velázquez et al., 2013; Willkofer et al., 2018). A thorough assessment of the contribution of the chain compartments to the overall uncertainty would require an ensemble of multiple climate and hydrological models.

455 The overall strong increase in frequency and intensity of the HF₁₀₀ in the future may be driven by deficiencies of the employed hydrological model, such as generalized glacier model among affected catchments, or a single snow melt approach for the entire Hydrological Bavaria (as described in Willkofer et al., 2020). However, as stated in the previous section, this scale of change was also found by Hattermann et al. (2018) for the upper Danube basin using the same emission scenario projections, but a different hydrological and climate model, which might indicate
460 that the change signals are likely independent of the chosen hydrological or climate model.

The results of the CCI on the frequency and intensity also depend on the performance of the hydrological model. Since it relies on observations for parameter calibration, the quality of this data is crucial, especially for extreme values. For the most extreme events (e.g., HF₁₀₀ and above) the river may inundate the surrounding area and the water level / discharge relationship at the gauging station used to determine discharge values may not be valid
465 anymore and is likely to underestimate the peak discharge. Therefore, the actual observed discharge – and thus, the calibrated model – is prone to these measurement uncertainties. Furthermore, the discharge of rivers within Hydrological Bavaria is heavily impacted by management structures for flood protection or hydro power generation, especially the southern tributaries of the Danube in the Alpine foreland and within the Alps are heavily regulated. Since the management follows somewhat fuzzy rules and actual data is restricted by private companies
470 in most cases, the management rules for these structures have to be deduced from publicly available data and implemented in the hydrological model. These rules are susceptible to extreme conditions as they do not allow for adaptations during model runtime (e.g., flushing a reservoir prior to an anticipated heavy precipitation event).

The projected future changes in extreme discharges may be attributed in part, to the climatological reference dataset, as it affects the performance of the hydrological model as well as the CCS through bias adjustment (Gampe et al., 2019; Meyer et al., 2019; Willkofer et al., 2018). Precipitation in high altitudes (e.g., the Alps) may be under-
475 captured (Westra et al., 2014; Poschlod, 2021; Prein and Gobiet, 2017; Rauthe et al., 2013; Poschlod et al., 2020; Willkofer et al., 2020) resulting in an underestimation of observed precipitation in these regions, especially of extreme values. Assuming a temporally stationary bias, changes in the extremes might be overestimated due to an over-adjustment of the distribution of the reference period towards underestimated observations compared to the
480 future periods. Furthermore, the variables are adjusted individually and thus, physical coherency as for a multivariate approach proposed by Meyer et al. (2019) is not guaranteed. This specifically affects discharges governed by snow or glacier melt of higher elevation within the Alps (Meyer et al., 2019).



485 Since the presented modelling approach only comprises one GCM-RCM combination forced by the more extreme RCP8.5 emission scenario as well as one hydrological model, the significance of the findings regarding the variance of change effects in the future on the development of extreme peak flows is limited. Furthermore, the projected climate change signals of the CRCM5-LE were found to depict a stronger warming and drying compared to other large ensembles (von Trentini et al., 2020) which might result in these part extreme increase in frequency and intensity of the HF₁₀₀ values among many gauges of Hydrological Bavaria.

490 Projected discharge extremes at the upper end of the distribution that have not been observed to date might be created by unrealistic compound events due to flaws in the bias correction approach (Kelder et al., 2022). Thus, these events directly influence the EVD, producing higher return values, and consequently, a larger change signal. However, as extreme precipitation events of various durations are expected to intensify within the studied region, the probability for yet unseen floods due to compounding events may also increase in the future.

5 Conclusion

495 This study emphasizes the benefit of employing a climatological SMILE with a hydrological model to create a hydro-SMILE to foster extreme value statistics and analyze the impacts of climate change on hydrological extreme values such as the HF₁₀₀ due to the provision of a very large database. This database allows for the application of empirical exceedance probabilities to estimate robust discharge values of high return periods rather than statistical extrapolation based on extreme value distributions. The results show that the performance of statistical estimates largely depends on the available length of the time series as well as its values when compared to the empirical benchmark. However, even with a length of 200 AM, the variance of the scatter of HF₁₀₀ estimates of the 1,000 samples was rather large.

505 As mentioned by Willkofer et al. (2020) the performance of the hydrological model allows for CCI studies - in this case using the CRCM5-LE to elaborate on the effects of climate change on the development of the HF₁₀₀. The projections reveal a strong increase in the intensity and frequency of HF₁₀₀ events for Alpine and pre-Alpine catchments exhibiting a snowmelt driven discharge regime within the reference period. This strong increase in the intensity and frequency is considerably smaller for catchments north of the Alps and of a more pluvial discharge regime. The in parts tremendous changes of HF₁₀₀ intensities and frequencies may be ascribed to the emission scenario (RCP8.5). Thus, the addition of different SMILEs and hydrological models may foster the significance of the findings due to different climate projections and simulated climatological and hydrological processes along the model chain. However, the establishment of such extensive model chains requires vast computational resources. Nevertheless, this effort should be considered regarding the benefits this profound database offers for



extreme value statistics, fostering the knowledge about the propagation of natural variability of the climate system to the hydrological response (Brunner et al., 2021b), or allowing to distinguish climate change signals (or forced response) from natural variability for extreme values (Wood and Ludwig, 2020; Aalbers et al., 2018).

Furthermore, the results highlight the need to incorporate climate projections in the design of new flood protection infrastructure or adapting existing structures to reduce future flood risk, not only in Hydrological Bavaria, but everywhere in general.

Contributions

515 FW developed the concept of this study including methods, investigation, and visualization, performed the formal analysis and validation, and prepared the original draft. FW and RRW were responsible for data curation and software development. RL acquired the funding for the presented research, provided the required resources, was responsible for the project administration, and supervised the presented research.

Competing interests:

525 The authors declare that they have no conflict of interest.

Acknowledgements:

The authors acknowledge the colleagues Gilbert Brietzke, André Kurzmann, and Jens Weismüller from Leibniz Supercomputing Centre of the Bavarian Academy of Sciences and Humanities for their technical support during the development of the hydrological large ensemble. We also thank the Leibniz Supercomputing Centre for providing the HPC infrastructure and computation time.

F.W. was supported by the ClimEx project, funded by the Bavarian Ministry for the Environment and Consumer Protection.

The CRCM5-LE was created within the ClimEx Project, which was funded by the Bavarian Ministry for the Environment and Consumer Protection. Computations of the CRCM5-LE were performed on the SuperMUC HPC system of the Leibniz Supercomputing Centre of the Bavarian Academy of Sciences and Humanities. We
535 acknowledge Environment and Climate Change Canada for providing the CanESM2-LE driving data.



References

- Aalbers, E. E., Lenderink, G., van Meijgaard, E., and van den Hurk, B. J. J. M.: Local-scale changes in mean and heavy precipitation in Western Europe, climate change or internal variability?, *Clim Dyn*, 50, 4745–4766, doi:10.1007/s00382-017-3901-9, 2018.
- Arora, V. K., Scinocca, J. F., Boer, G. J., Christian, J. R., Denman, K. L., Flato, G. M., Khari, V. V., Lee, W. G., and Merryfield, W. J.: Carbon emission limits required to satisfy future representative concentration pathways of greenhouse gases, *Geophys. Res. Lett.*, 38, L05805, doi:10.1029/2010GL046270, 2011.
- Bertola, M., Viglione, A., Lun, D., Hall, J., and Blöschl, G.: Flood trends in Europe: are changes in small and big floods different?, *Hydrol. Earth Syst. Sci.*, 24, 1805–1822, doi:10.5194/hess-24-1805-2020, 2020.
- Bezák, N., Brilly, M., and Šraj, M.: Comparison between the peaks-over-threshold method and the annual maximum method for flood frequency analysis, *Hydrological Sciences Journal*, 59, 959–977, doi:10.1080/02626667.2013.831174, 2014.
- BGR: International Hydrogeological Map of Europe 1:1,500,000 (IHME1500 v1.1), Bundesanstalt für Geowissenschaften und Rohstoffe (BGR), Hannover, Germany, Paris, France, 2014.
- Blöschl, G., Gaál, L., Hall, J., Kiss, A., Komma, J., Nester, T., Parajka, J., Perdigão, R. A. P., Plavcová, L., Rogger, M., Salinas, J. L., and Viglione, A.: Increasing river floods: fiction or reality?, *WIREs Water*, 2, 329–344, doi:10.1002/wat2.1079, 2015.
- Blöschl, G., Hall, J., Viglione, A., Perdigão, R. A. P., Parajka, J., Merz, B., Lun, D., Arheimer, B., Aronica, G. T., Bilibashi, A., Boháč, M., Bonacci, O., Borga, M., Čanjevac, I., Castellarin, A., Chirico, G. B., Claps, P., Frolova, N., Ganora, D., Gorbachova, L., Gül, A., Hannaford, J., Harrigan, S., Kireeva, M., Kiss, A., Kjeldsen, T. R., Kohnová, S., Koskela, J. J., Ledvinka, O., Macdonald, N., Mavrova-Guirguinova, M., Mediero, L., Merz, R., Molnar, P., Montanari, A., Murphy, C., Osuch, M., Ovcharuk, V., Radevski, I., Salinas, J. L., Sauquet, E., Šraj, M., Szolgay, J., Volpi, E., Wilson, D., Zaimi, K., and Živković, N.: Changing climate both increases and decreases European river floods, *Nature*, 573, 108–111, doi:10.1038/s41586-019-1495-6, 2019.
- Blöschl, G., Nester, T., Komma, J., Parajka, J., and Perdigão, R. A. P.: The June 2013 flood in the Upper Danube Basin, and comparisons with the 2002, 1954 and 1899 floods, *Hydrol. Earth Syst. Sci.*, 17, 5197–5212, doi:10.5194/hess-17-5197-2013, 2013.
- Brunner, M. I., Slater, L., Tallaksen, L. M., and Clark, M.: Challenges in modeling and predicting floods and droughts: A review, *WIREs Water*, 8, doi:10.1002/wat2.1520, 2021a.



- Brunner, M. I., Swain, D. L., Wood, R. R., Willkofer, F., Done, J. M., Gilleland, E., and Ludwig, R.: An extremeness threshold determines the regional response of floods to changes in rainfall extremes, *Commun Earth Environ*, 2, doi:10.1038/s43247-021-00248-x, 2021b.
- 570 Černý, V.: Thermodynamical approach to the traveling salesman problem: An efficient simulation algorithm, *J Optim Theory Appl*, 45, 41–51, doi:10.1007/BF00940812, 1985.
- Champagne, O., Leduc, M., Coulibaly, P., and Arain, M. A.: Winter hydrometeorological extreme events modulated by large-scale atmospheric circulation in southern Ontario, *Earth Syst. Dynam.*, 11, 301–318, doi:10.5194/esd-11-301-2020, 2020.
- 575 Chen, J., Arsenault, R., Brissette, F. P., and Zhang, S.: Climate Change Impact Studies: Should We Bias Correct Climate Model Outputs or Post-Process Impact Model Outputs?, *Water Resour. Res.*, 57, doi:10.1029/2020WR028638, 2021.
- Dettinger, M. D., Cayan, D. R., Meyer, M. K., and Jeton, A. E.: Simulated Hydrologic Responses to Climate Variations and Change in the Merced, Carson, and American River Basins, Sierra Nevada, California, 1900–
- 580 2099, *Climatic Change*, 62, 283–317, doi:10.1023/B:CLIM.0000013683.13346.4f, 2004.
- Dörhöfer, G., Hannappel, S., Reutter, E., and Voigt, H.-J.: Die Hydrogeologische Übersichtskarte von Deutschland HÜK200, *Z. Für Angew. Geol.*, 153–159, 2001.
- Ehmele, F., Kautz, L.-A., Feldmann, H., and Pinto, J. G.: Long-term variance of heavy precipitation across central Europe using a large ensemble of regional climate model simulations, *Earth Syst. Dynam.*, 11, 469–490,
- 585 doi:10.5194/esd-11-469-2020, 2020.
- Ehret, U., Zehe, E., Wulfmeyer, V., Warrach-Sagi, K., and Liebert, J.: HESS Opinions "Should we apply bias correction to global and regional climate model data?", *Hydrol. Earth Syst. Sci.*, 16, 3391–3404, doi:10.5194/hess-16-3391-2012, 2012.
- European Environment Agency: Corine Land Cover 2006 v17, [https://www.eea.europa.eu/data-and-](https://www.eea.europa.eu/data-and-maps/data/clc-2006-raster-3)
- 590 [maps/data/clc-2006-raster-3](https://www.eea.europa.eu/data-and-maps/data/clc-2006-raster-3), 2013a.
- European Environment Agency: Digital Elevation Model over Europe (EU-DEM), <https://www.eea.europa.eu/data-and-maps/data/eu-dem>, 2013b.
- Fischer, S. and Schumann, A.: Robust flood statistics: comparison of peak over threshold approaches based on monthly maxima and TL-moments, *Hydrological Sciences Journal*, 61, 457–470,
- 595 doi:10.1080/02626667.2015.1054391, 2016.
- Fyfe, J. C., Derksen, C., Mudryk, L., Flato, G. M., Santer, B. D., Swart, N. C., Molotch, N. P., Zhang, X., Wan, H., Arora, V. K., Scinocca, J., and Jiao, Y.: Large near-term projected snowpack loss over the western United States, *Nature communications*, 8, 14996, doi:10.1038/ncomms14996, 2017.



- 600 Gampe, D., Schmid, J., and Ludwig, R.: Impact of Reference Dataset Selection on RCM Evaluation, Bias
Correction, and Resulting Climate Change Signals of Precipitation, *Journal of Hydrometeorology*, 20, 1813–
1828, doi:10.1175/JHM-D-18-0108.1, 2019.
- Gilleland, E. and Katz, R. W.: extRemes 2.0: An Extreme Value Analysis Package in R, *J. Stat. Soft.*, 72,
doi:10.18637/jss.v072.i08, 2016.
- 605 GRDC: Summary Statistics by Country,
https://www.bafg.de/SharedDocs/ExterneLinks/GRDC/summary_stat_cc_pdf.pdf?__blob=publicationFile,
2021.
- Gupta, H. V., Kling, H., Yilmaz, K. K., and Martinez, G. F.: Decomposition of the mean squared error and NSE
performance criteria: Implications for improving hydrological modelling, *Journal of Hydrology*, 377, 80–91,
doi:10.1016/j.jhydrol.2009.08.003, 2009.
- 610 Hattermann, F. F., Wortmann, M., Liersch, S., Toumi, R., Sparks, N., Genillard, C., Schröter, K., Steinhausen, M.,
Gyalai-Korpos, M., Máté, K., Hayes, B., del Rocío Rivas López, M., Rácz, T., Nielsen, M. R., Kaspersen, P.
S., and Drews, M.: Simulation of flood hazard and risk in the Danube basin with the Future Danube Model,
Climate Services, 12, 14–26, doi:10.1016/j.cliser.2018.07.001, 2018.
- 615 Haylock, M. R., Hofstra, N., Klein Tank, A. M. G., Klok, E. J., Jones, P. D., and New, M.: A European daily high-
resolution gridded data set of surface temperature and precipitation for 1950–2006, *J. Geophys. Res.*, 113,
doi:10.1029/2008JD010201, 2008.
- Huang, S., Krysanova, V., and Hattermann, F. F.: Does bias correction increase reliability of flood projections
under climate change? A case study of large rivers in Germany, *Int. J. Climatol.*, 34, 3780–3800,
doi:10.1002/joc.3945, 2014.
- 620 Iacob, O., Brown, I., and Rowan, J.: Natural flood management, land use and climate change trade-offs: the case
of Tarland catchment, Scotland, *Hydrological Sciences Journal*, 62, 1931–1948,
doi:10.1080/02626667.2017.1366657, 2017.
- IPCC: Summary for Policymakers, in: *Climate Change 2021: The Physical Science Basis. Contribution of
Working Group I to the Sixth Assessment Report of the Intergovernmental Panel on Climate Change*, Masson-
625 Delmotte, V., Zhai, P., Pirani, A., Connors, S. L., Péan, C., Berger, S., Caud, N., Chen, Y., Goldfarb, L.,
Gomis, M. I., Huang, M., Leitzell, K., Lonnoy, E., Matthews, J. B. R., Maycock, T. K., Waterfield, T., Yelekçi,
O., Yu, R., Zhou, B. (Eds.), In Press., 2021.
- JÓNSDÓTTIR, J. F.: A runoff map based on numerically simulated precipitation and a projection of future runoff
in Iceland / Une carte d'écoulement basée sur la précipitation numériquement simulée et un scénario du futur
630 écoulement en Islande, *Hydrological Sciences Journal*, 53, 100–111, doi:10.1623/hysj.53.1.100, 2008.



- Kelder, T., Wanders, N., van der Wiel, K., Marjoribanks, T. I., Slater, L. J., Wilby, R. I., and Prudhomme, C.: Interpreting extreme climate impacts from large ensemble simulations—are they unseen or unrealistic?, *Environ. Res. Lett.*, 17, 44052, doi:10.1088/1748-9326/ac5cf4, 2022.
- Kendon, E. J., Rowell, D. P., Jones, R. G., and Buonomo, E.: Robustness of Future Changes in Local Precipitation
635 Extremes, *J. Climate*, 21, 4280–4297, doi:10.1175/2008JCLI2082.1, 2008.
- Kirchmeier-Young, M. C., Zwiers, F. W., and Gillett, N. P.: Attribution of Extreme Events in Arctic Sea Ice Extent, *J. Climate*, 30, 553–571, doi:10.1175/JCLI-D-16-0412.1, 2017.
- Kirkpatrick, S., Gelatt, C. D., and Vecchi, M. P.: Optimization by simulated annealing, *Science (New York, N.Y.)*, 220, 671–680, doi:10.1126/science.220.4598.671, 1983.
- 640 Kjellström, E., Thejll, P., Rummukainen, M., Christensen, J. H., Boberg, F., Christensen, O. B., and Fox Maule, C.: Emerging regional climate change signals for Europe under varying large-scale circulation conditions, *Clim. Res.*, 56, 103–119, doi:10.3354/cr01146, 2013.
- Leduc, M., Mailhot, A., Frigon, A., Martel, J.-L., Ludwig, R., Brietzke, G. B., Giguère, M., Brissette, F., Turcotte, R., Braun, M., and Scinocca, J.: The ClimEx Project: A 50-Member Ensemble of Climate Change Projections
645 at 12-km Resolution over Europe and Northeastern North America with the Canadian Regional Climate Model (CRCM5), *Journal of Applied Meteorology and Climatology*, 58, 663–693, doi:10.1175/JAMC-D-18-0021.1, 2019.
- Ludwig, R., Wood, Raul, R., Willkofer, F., von Trentini, F., Mittermeier, M., Böhnisch, A., and Poschlod, B.: ClimEx - Klimawandel und Extremereignisse: Risiken und Perspektiven für die bayerische Wasserwirtschaft, Abschlussbericht, Ludwig-Maximilians-Universität, 190 pp., 2019.
- 650 Maher, N., Milinski, S., and Ludwig, R.: Large ensemble climate model simulations: introduction, overview, and future prospects for utilising multiple types of large ensemble, *Earth Syst. Dynam.*, 12, 401–418, doi:10.5194/esd-12-401-2021, 2021.
- Maraun, D.: Bias Correcting Climate Change Simulations - a Critical Review, *Curr Clim Change Rep*, 2, 211–
655 220, doi:10.1007/s40641-016-0050-x, 2016.
- Martel, J.-L., Mailhot, A., and Brissette, F.: Global and Regional Projected Changes in 100-yr Subdaily, Daily, and Multiday Precipitation Extremes Estimated from Three Large Ensembles of Climate Simulations, *J. Climate*, 33, 1089–1103, doi:10.1175/JCLI-D-18-0764.1, 2020.
- Martel, J.-L., Mailhot, A., Brissette, F., and Caya, D.: Role of Natural Climate Variability in the Detection of
660 Anthropogenic Climate Change Signal for Mean and Extreme Precipitation at Local and Regional Scales, *J. Climate*, 31, 4241–4263, doi:10.1175/JCLI-D-17-0282.1, 2018.



- Martynov, A., Laprise, R., Sushama, L., Winger, K., Šeparović, L., and Dugas, B.: Reanalysis-driven climate simulation over CORDEX North America domain using the Canadian Regional Climate Model, version 5: model performance evaluation, *Clim Dyn*, 41, 2973–3005, doi:10.1007/s00382-013-1778-9, 2013.
- 665 Meyer, J., Kohn, I., Stahl, K., Hakala, K., Seibert, J., and Cannon, A. J.: Effects of univariate and multivariate bias correction on hydrological impact projections in alpine catchments, *Hydrol. Earth Syst. Sci.*, 23, 1339–1354, doi:10.5194/hess-23-1339-2019, 2019.
- Mittermeier, M., Braun, M., Hofstätter, M., Wang, Y., and Ludwig, R.: Detecting Climate Change Effects on Vb Cyclones in a 50-Member Single-Model Ensemble Using Machine Learning, *Geophys. Res. Lett.*, 46, 14653–
670 14661, doi:10.1029/2019GL084969, 2019.
- Moriasi, D. N., Arnold, J. G., van Liew, M. W., Bingner, R. L., Harmel, R. D., and Veith, T. L.: Model Evaluation Guidelines for Systematic Quantification of Accuracy in Watershed Simulations, *Transactions of the ASABE*, 50, 885–900, doi:10.13031/2013.23153, 2007.
- Mpelasoka, F. S. and Chiew, F. H. S.: Influence of Rainfall Scenario Construction Methods on Runoff Projections, *Journal of Hydrometeorology*, 10, 1168–1183, doi:10.1175/2009JHM1045.1, 2009.
- 675 Muerth, M., Gauvin St-Denis, B., Ludwig, R., and Caya, D.: Evaluation of different sources of uncertainty in climate change impact research using a hydro-climatic model ensemble, *International Congress on Environmental Modelling and Software*, doi:10.5282/ubm/epub.14094, 2012.
- Muerth, M. J., Gauvin St-Denis, B., Ricard, S., Velázquez, J. A., Schmid, J., Minville, M., Caya, D., Chaumont, D., Ludwig, R., and Turcotte, R.: On the need for bias correction in regional climate scenarios to assess climate
680 change impacts on river runoff, *Hydrol. Earth Syst. Sci.*, 17, 1189–1204, doi:10.5194/hess-17-1189-2013, 2013.
- Nash, J. E. and Sutcliffe, J. V.: River flow forecasting through conceptual models part I — A discussion of principles, *Journal of Hydrology*, 10, 282–290, doi:10.1016/0022-1694(70)90255-6, 1970.
- 685 Neukum, C. and Azzam, R.: Impact of climate change on groundwater recharge in a small catchment in the Black Forest, Germany, *Hydrogeol J*, 20, 547–560, doi:10.1007/s10040-011-0827-x, 2012.
- Poschlod, B.: Using high-resolution regional climate models to estimate return levels of daily extreme precipitation over Bavaria, [preprint], *Nat. Hazards Earth Syst. Sci. Discuss*, doi:10.5194/nhess-2021-66, 2021.
- Poschlod, B., Willkofer, F., and Ludwig, R.: Impact of Climate Change on the Hydrological Regimes in Bavaria, *Water*, 12, 1599, doi:10.3390/w12061599, 2020.
- 690 Prein, A. F. and Gobiet, A.: Impacts of uncertainties in European gridded precipitation observations on regional climate analysis, *Int. J. Climatol.*, 37, 305–327, doi:10.1002/joc.4706, 2017.



- Rauthe, M., Steiner, H., Riediger, U., Mazurkiewicz, A., and Gratzki, A.: A Central European precipitation climatology – Part I: Generation and validation of a high-resolution gridded daily data set (HYRAS), *metz*, 22, 235–256, doi:10.1127/0941-2948/2013/0436, 2013.
- 695
- Salinas, J. L., Castellarin, A., Viglione, A., Kohnová, S., and Kjeldsen, T. R.: Regional parent flood frequency distributions in Europe – Part 1: Is the GEV model suitable as a pan-European parent?, *Hydrol. Earth Syst. Sci.*, 18, 4381–4389, doi:10.5194/hess-18-4381-2014, 2014.
- Schulla, J.: Model Description WaSiM (Water balance Simulation Model), Zurich, 2021.
- 700
- Schulz, K. and Bernhardt, M.: The end of trend estimation for extreme floods under climate change?, *Hydrol. Process.*, 30, 1804–1808, doi:10.1002/hyp.10816, 2016.
- Šeparović, L., Alexandru, A., Laprise, R., Martynov, A., Sushama, L., Winger, K., Tete, K., and Valin, M.: Present climate and climate change over North America as simulated by the fifth-generation Canadian regional climate model, *Clim Dyn*, 41, 3167–3201, doi:10.1007/s00382-013-1737-5, 2013.
- 705
- Sigmond, M., Fyfe, J. C., and Swart, N. C.: Ice-free Arctic projections under the Paris Agreement, *Nature Clim Change*, 8, 404–408, doi:10.1038/s41558-018-0124-y, 2018.
- Stahl, N. and Hofstätter, M.: Vb-Zugbahnen und deren Auftreten als Serie mit Bezug zu den resultierenden Hochwassern in Bayern und Auswirkungen auf Rückhalteräume im Isareinzugsgebiet, *Hydrologie und Wasserbewirtschaftung*, 62, 77–97, doi:10.5675/HyWa_2018,2_2, 2018.
- 710
- Teutschbein, C. and Seibert, J.: Bias correction of regional climate model simulations for hydrological climate-change impact studies: Review and evaluation of different methods, *Journal of Hydrology*, 456–457, 12–29, doi:10.1016/j.jhydrol.2012.05.052, 2012.
- Thielen, A. H., Kienzler, S., Kreibich, H., Kuhlicke, C., Kunz, M., Mühr, B., Müller, M., Otto, A., Petrow, T., Pisi, S., and Schröter, K.: Review of the flood risk management system in Germany after the major flood in 2013, *E&S*, 21, doi:10.5751/ES-08547-210251, 2016.
- 715
- Tolson, B. A. and Shoemaker, C. A.: Dynamically dimensioned search algorithm for computationally efficient watershed model calibration, *Water Resour. Res.*, 43, doi:10.1029/2005WR004723, 2007.
- van Vuuren, D. P., Edmonds, J., Kainuma, M., Riahi, K., Thomson, A., Hibbard, K., Hurtt, G. C., Kram, T., Krey, V., Lamarque, J.-F., Masui, T., Meinshausen, M., Nakicenovic, N., Smith, S. J., and Rose, S. K.: The representative concentration pathways: an overview, *Climatic Change*, 109, 5–31, doi:10.1007/s10584-011-0148-z, 2011.
- 720
- Velázquez, J. A., Schmid, J., Ricard, S., Muerth, M. J., Gauvin St-Denis, B., Minville, M., Chaumont, D., Caya, D., Ludwig, R., and Turcotte, R.: An ensemble approach to assess hydrological models' contribution to



- 725 uncertainties in the analysis of climate change impact on water resources, *Hydrol. Earth Syst. Sci.*, 17, 565–
578, doi:10.5194/hess-17-565-2013, 2013.
- von Trentini, F., Aalbers, E. E., Fischer, E. M., and Ludwig, R.: Comparing interannual variability in three regional
single-model initial-condition large ensembles (SMILEs) over Europe, *Earth Syst. Dynam.*, 11, 1013–1031,
doi:10.5194/esd-11-1013-2020, 2020.
- 730 Westra, S., Fowler, H. J., Evans, J. P., Alexander, L. V., Berg, P., Johnson, F., Kendon, E. J., Lenderink, G., and
Roberts, N. M.: Future changes to the intensity and frequency of short-duration extreme rainfall, *Rev.
Geophys.*, 52, 522–555, doi:10.1002/2014RG000464, 2014.
- Wilhelm, B., Rapuc, W., Amann, B., Anselmetti, F. S., Arnaud, F., Blanchet, J., Brauer, A., Czymzik, M., Giguet-
Covex, C., Gilli, A., Glur, L., Grosjean, M., Irmeler, R., Nicolle, M., Sabatier, P., Swierczynski, T., and Wirth,
S. B.: Impact of warmer climate periods on flood hazard in the European Alps, *Nat. Geosci.*, 15, 118–123,
735 doi:10.1038/s41561-021-00878-y, 2022.
- Willkofer, F., Schmid, F.-J., Komischke, H., Korck, J., Braun, M., and Ludwig, R.: The impact of bias correcting
regional climate model results on hydrological indicators for Bavarian catchments, *Journal of Hydrology:
Regional Studies*, 19, 25–41, doi:10.1016/j.ejrh.2018.06.010, 2018.
- 740 Willkofer, F., Wood, R. R., Trentini, F. von, Weismüller, J., Poschlod, B., and Ludwig, R.: A Holistic Modelling
Approach for the Estimation of Return Levels of Peak Flows in Bavaria, *Water*, 12, 2349,
doi:10.3390/w12092349, 2020.
- Wood, R. R., Lehner, F., Pendergrass, A. G., and Schlunegger, S.: Changes in precipitation variability across time
scales in multiple global climate model large ensembles, *Environ. Res. Lett.*, doi:10.1088/1748-9326/ac10dd,
2021.
- 745 Wood, R. R. and Ludwig, R.: Analyzing Internal Variability and Forced Response of Subdaily and Daily Extreme
Precipitation Over Europe, *Geophys. Res. Lett.*, 47, doi:10.1029/2020GL089300, 2020.